Available online at www.sciencedirect.com
ScienceDirect
Journal of Chromatography B, 848 (2007) 131–141
JOURNAL OF CHROMATOGRAPHY B
www.elsevier.com/locate/chromb

Lumped parameter model for prediction of initial breakthrough profiles for the chromatographic capture of antibodies from a complex feedstock☆

Hanne Bak[a,c,1], Owen R.T. Thomas[a,d], Jens Abildskov[b,*]

[a] *Center for Microbial Biotechnology, BioCentrum-DTU, Technical University of Denmark, Building 223, Søltofts Plads, DK-2800 Kgs. Lyngby, Denmark*
[b] *Computer-Aided Process Engineering Center, Department of Chemical Engineering, Technical University of Denmark, Building 229, DK-2800 Kgs. Lyngby, Denmark*
[c] *DakoCytomation A/S, Produktionsvej 42, DK-4600 Glostrup, Denmark*
[d] *Department of Chemical Engineering, The University of Birmingham, Edgbaston, Birmingham B15 2TT, UK*

Received 3 April 2006; accepted 18 July 2006
Available online 21 August 2006

Abstract

A simple mathematical model to predict initial breakthrough profiles from preparative chromatographic separations of biological macromolecules has been developed. A lumped parameter approach was applied, employing Langmuirian adsorption kinetics to describe the rate of mass transfer (MT) from the bulk liquid in the column to the bound state. Equilibrium and kinetic adsorption data were determined for six different packed bed chromatographic adsorbents: two derivatised with rProtein A; and four functionalised with synthetic low molecular weight ligands. All adsorption isotherms were well described by the Langmuir model, whereas the data fitting to kinetic batch experiments showed that the model was inadequate after the first ∼25 min of adsorption for four of the six adsorbents. The model underestimated the dynamic Ig breakthough on packed beds of rProtein A Sepharose FF, MabSelect, MBI HyperCel, and MabSorbent A1P, applying a feedstock of 20–100% (v/v) clarified rabbit antiserum. However, when employing a maximum adsorption capacity 25% greater than that determined in batch binding studies, excellent agreement was obtained at all antiserum strengths for most adsorbents. Useful insights into scale-up and process design can be obtained by applying the model, without determining tentative parameters specific for each adsorbent and target protein concentration. However, the model parameters are solvent dependent so a prerequisite for its true applicability is that binding is both Langmuirian and essentially independent of the ionic strength of the feedstock applied.

Keywords: Biomimetic ligands; Hydrophobic charge induction; Immunoglobulin purification; Mixed mode adsorbents; Modelling; Protein A affinity adsorption

1. Introduction

Today, optimisation and to some extent scale-up of chromatographic processes, are mostly performed empirically. However, within the last two decades various mathematical models have been developed describing the breakthrough behaviour of a range of chromatographic systems, such as hydrophobic interaction [1], dye ligand affinity [2,3], ion-exchange [4], and affinity [5,6]. These models can provide an understanding of the equilibrium and mass transfer (MT) characteristics of an adsorbent, and consequently represents powerful tools for targeted optimisation and scale-up.

The major differences between the various models lie in the description of the mass transport limitations of the protein from the bulk liquid in the column to the bound state. As shown in Fig. 1, the overall mass transfer resistance is resolved into contributions associated with:

(i) mass transfer from bulk liquid to the liquid boundary layer around the adsorbent particles;
(ii) MT through the boundary layer;

Abbreviations: CIP, cleaning in place; HCI, hydrophobic charge induction; Ig, immunoglobulin; IgG, immunoglobulin G; MT, mass transfer; RTD, residence time distribution

☆ This paper is part of a special issue entitled "Polyclonal and Monoclonal Antibody Production, Purification, Process and Product Analytics", guest edited by A.R. Newcombe and K. Watson.

* Corresponding author. Tel.: +45 45252905; fax: +45 45932906.
E-mail address: ja@kt.dtu.dk (J. Abildskov).
[1] Present address: Regeneron Pharmaceuticals Inc., Preclinical Manufacturing and Process Development, 777 Old Saw Mill River Road, Tarrytown, NY 10591, USA.

1570-0232/$ – see front matter © 2006 Elsevier B.V. All rights reserved.
doi:10.1016/j.jchromb.2006.07.020

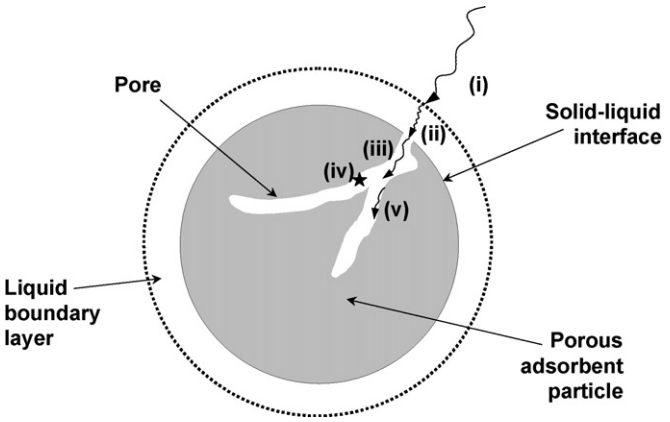

Fig. 1. The discrete mass transport steps involved in the transport of target protein from the bulk liquid in the column to the bound state: (i) mass transfer (MT) from the bulk liquid to the liquid boundary layer around the adsorbents particle; (ii) MT through the boundary layer; (iii) transfer through the pores of the adsorbent particles; (iv) adsorption kinetics; (v) surface diffusion along the internal pore surface. Image redrawn from [7].

(iii) transfer through pores of the adsorbent particles;
(iv) adsorption kinetics; and
(v) surface diffusion along the internal pore surface of the adsorbent particles.

Very similar overall mass balances are applied in the published models, and the majority of these employ the Langmuir adsorption isotherm [1–3,5,6,8,9] for describing the non-linear favourable kinetics, typically observed with most proteins.

Sophisticated models, taking film, pore, or surface diffusion (or various combinations) into account, have been developed [1,5,6,8]. However, all of these require determination of a large number of parameters, either experimentally, or calculated from approximation equations based on strongly simplified assumptions regarding the geometry of adsorbate and adsorbent. If the adsorbate/adsorbent is difficult to characterize geometrically, one may employ related expressions, but include these as parameters to be determined from data fits.

Most work done so far on development of models describing chromatographic processes has been performed with mono- [3,5,6,8,9] or bi- [10] component systems, and in only one report was a multi-component system analysed, i.e. for the adsorption of lipase from a fermentation broth [1]. Such 'ideal system' based models are unlikely to find widespread industrial application.

Attempts have been made with two-component systems [10,11] to develop models of batch adsorption isotherms, incorporating the competition between molecules, where parameter determination was performed in pure solutions. However, applying this approach to a complex feedstock would require individual parameters to be determined for each component, or a number of the main contaminants in addition to the target molecule, again potentially leading to lengthy computations, and limiting the direct application of such models.

The work described here entails direct capture of the target molecule from a complex clarified feedstock. This has been chosen in order to avoid using model solutions and thus more closely mimics a real system, which potentially makes it a model of interest in an industrial framework. The model system comprises clarified rabbit antiserum and a number of commercially available and prototype adsorbents designed for direct capture of antibodies. Two of these materials featured rProtein A (rProtein A Sepharose and MabSelect) as the ligand. These differed from each other with respect to underlying base matrix and ligand density. The remaining four matrices comprised various synthetic low molecular weight ligands immobilised on hydrophilic porous supports and these included: MabSorbent A1P; MEP HyperCel; MBI HyperCel; and MNA HyperCel (see Table 1 for detailed descriptions).

In studying adsorption of serum proteins to packed bed chromatographic media, pore and film diffusion were shown to be rate limiting in systems comprising: (i) bovine serum albumin (BSA) and S Sepharose FF [4]; (ii) immunoglobulin G (IgG) and Protein A Sepharose FF [5]; and (iii) IgG and BSA on ion-exchangers [8]. Good fits of the initial breakthrough in frontal analysis were obtained, regardless of whether a lumped parameter approach was taken, or whether film and pore diffusion were included in the 'BSA and S Sepharose FF' [4] system. This analysis was not performed with any of the IgG systems studied [5,8]. However, studies of IgG penetration in SP Sepharose FF during batch adsorption employing confocal microscopy, showed that only a small fraction of IgG had diffused into the adsorbent particle after 0.5 h [18], therefore, limiting the effect of pore diffusion on initial breakthrough predictions.

Based on the above, the working hypothesis applied in the current study was as follows. In order to obtain a first estimate of Ig breakthrough on packed bed adsorbents, a simple model with a lumped parametric approach would be sufficient (Fig. 2). The parameters for the model were determined by kinetic and equilibrium batch adsorption studies, employing a complex feedstock, i.e. undiluted clarified rabbit antiserum, and the dynamic model was applied for frontal analysis over a range of feedstock strengths (i.e., 20–100%, v/v rabbit antiserum).

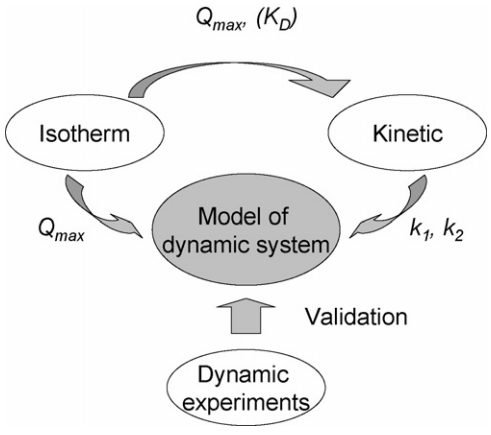

Fig. 2. Generation of a predictive mathematical model of a preparative chromatographic process with a lumped parameter approach: (i) an isotherm is generated, and the parameters Q_{max} and K_D are found through fitting the data to a Langmuir Isotherm; (ii) Q_{max} (and K_D) are used to fit the kinetic expression, generating the parameters k_1 and k_2; (iii) Q_{max}, k_1, k_2 are then used in the mathematical model of the dynamic system; (iv) comparing the model to experimentally obtained breakthrough curves subsequently validates this model.

Table 1
Description of adsorbents employed in this study

Adsorbent	Immobilised ligand	Description of base particle	Manufacturer
rProtein A Sepharose FF	Recombinant Protein A[a] (lot no. 279973, 6 mg mL^{-1})	60–165 μm highly cross-linked 4% agarose	GE Healthcare, Uppsala, Sweden
MabSelect	Recombinant Protein A[a] (lot no. 286511, 5 mg mL^{-1})	40–130 μm (av. 85 μm) highly cross-linked rigid 'HF' 3.5% agarose base matrix[b]	GE Healthcare, Uppsala, Sweden
MabSorbents A1P	Mimic of key dipeptide motif in Protein A[c,d] (lot no. FA0415)	75–125 μm highly cross-linked 6% agarose base matrix	Prometic Biosciences Ltd., Cambridge, UK
MEP HyperCel	4-mercapto-ethyl-pyridine (lot no. A112, 100 μmol mL^{-1})[e]	Av. 90 ± 10 μm cellulosic base matrix	Pall Corporation, BioSepra Process Division, Cergy-Saint-Christophe, France
MBI HyperCel	mercapto-benzimidazole-sulphonic-acid (lot no.'s 00901 and EA040402B, 94 and 51 μmol mL^{-1}, respectively)[f]	Av. 90 ± 10 μm cellulosic base matrix	Pall Corporation, BioSepra Process Division, Cergy-Saint-Christophe, France
MNA HyperCel	mercapto-nicotinic-acid (lot no.'s S1001 and A2001, 58 and 40 μmol mL^{-1}, respectively)[f]	Av. 90 ± 10 μm cellulosic base matrix	Pall Corporation, BioSepra Process Division, Cergy-Saint-Christophe, France

[a] Engineered to include C-terminal cysteine allowing oriented coupling via thioether linkage through a stable 12-atom epoxide spacer arm to the base matrix (ensuring low ligand leakage).
[b] Rigid agarose support cross-linked (technique undisclosed) to allow high flow rates under process conditions.
[c] Ligand (structure not disclosed) comprises a triazine scaffold with two spatially oriented substituents that mimic the helical twist of the key dipeptide in Protein A [12].
[d] The ligand density is proprietary to the producer.
[e] Binding relies on salt-independent hydrophobic interaction, whereas elution is mediated by pH induced electrostatic repulsion, hence the term 'hydrophobic charge induction' (HCI) [13–17].
[f] Prototype adsorbents featuring ligands loosely described by the manufacturer as being of the 'HCI class'.

2. Theory

2.1. The model

The overall mass balance is based on the equation of continuity of isothermal adsorption of a single solute in plug flow through a packed bed of monodisperse porous particles, including axial dispersion based on Fickian molecular diffusion theory [1,7,19]. It is a common practice to solve such models with 'Danckwertz boundary conditions' [20], where the spatial derivative of the dependent variables are required to be zero at the bed exit, even though this condition is debatable under non-steady state conditions. A parameter investigation showed that axial dispersion had a negligible influence on the shape and position of the breakthrough curve. This was supported [21] by a parametric study of an affinity system, and many other workers have applied the assumption that axial dispersion is negligible in packed bed simulations [2,3,5,7]. Initially film diffusion was included in our model. However, a parameter investigation showed that the solid surface concentration of the adsorbent was almost always close to the bulk concentration, indicating limited mass transport resistance by film diffusion in the dynamic model. On this basis, film diffusion was regarded as negligible. Thus, going beyond the Langmuir model would increase the mathematical complexity, but might not necessarily improve the predictive power of the model, since the extension was not qualified by physical considerations.

In summary, the data fitting presented below here was performed assuming film diffusion and axial dispersion as negligible, applying Eq. (1):

$$\frac{\partial C}{\partial t} = -u\frac{\partial C}{\partial z} - \left(\frac{1-\varepsilon}{\varepsilon}\right)\frac{\partial Q}{\partial t} \quad (1)$$

where C is the concentration of target protein in the bulk liquid phase. Q is the amount of target protein adsorbed, t is time, u the interstitial linear velocity, z the bed depth/length, and ε is the void fraction of the bed. Furthermore, the choice of applying Eq. (1) has the advantage of eliminating the need for Danckwertz boundary conditions. Thus, the boundary condition becomes $C(0,t) = C_0$. The initial condition is $Q(z,0) = 0$. Values for ε were calculated for each adsorbent with Eq. (2) [22–24]:

$$\varepsilon = 1 - \frac{V_0(1-\varepsilon_0)}{V} \quad (2)$$

with V_0 and V being the settled bed volume and packed bed volume respectively, and ε_0 the voidage of the settled bed. $\varepsilon_0 = 0.4$ was assumed for all adsorbents, as this value has been reported for a range of chromatographic media with particle sizes ranging from 32 to 550 μm [22–26].

The ε values determined in the current study (Table 2) are lower than those that have been reported for other systems [1,21,27,28], and are close to $\varepsilon = 0.27$, which is the number for ideally packed, rigid, incompressible, monodisperse supports [29]. In all of the aforementioned studies however, significantly lower flow rates were applied than those employed in this work. Given that the particles applied in this study were compressible and exhibit relatively large size distributions the values obtained seem reasonable; moreover they lie within the reported range [23].

Table 2
Chromatographic and Langmuir parameters for all adsorbents used in the dynamic model.

Adsorbent	L (cm)[a]	ε[b]	Q_{max} (mg g^{-1})[c]	K_D (μM)[d]	$K_D = \frac{k_2}{k_1}$	k_1, k_2 independent			
					$k_1 \times 10^3$ (L g^{-1} min^{-1})	$k_2 \times 10^2$ (min^{-1})	$k_1 \times 10^3$ (L g^{-1} min^{-1})	$k_2 \times 10^2$ (min^{-1})	K_D (μM)[e]
rProtein A Sepharose FF	5.8	0.24	72.5	3.1	17.7	0.85	21.0	3.22	10.2
MabSelect	6.5	0.26	57.5	3.0	50.1	2.3	57.0	7.8	9.1
MabSorbent A1P	6.4	0.27	31.6	23.3	41.2	14.4	43.0	22.4	34.7
MEP HyperCel	7.3, 6.4[f]	0.28	81.5	13.3	4.45	0.89	4.98	2.18	29.2
MBI HyperCel	7.0	0.28	50.6	12.7	13.0	2.5	24.7	15.4	41.6
MNA HyperCel	7.3	0.28	46.5	8.0	2.8	0.33	4.1	3.3	53.7

[a] Internal column diameter = 10 mm.
[b] Determined by Eq. (2).
[c] It was experimentally validated for all adsorbents but MabSorbent A1P, that Q_{max} in mg Ig per mL packed adsorbent equals the Q_{max} mg Ig per g suction dried adsorbent found in the adsorption isotherms.
[d] Determined from the adsorption isotherms (Fig. 3) by least square fits of Eq. (4) with Origin 4.1.
[e] Calculated from $K_D = k_2/k_1$, where k_1 and k_2 were determined as independent parameters with Eq. (3).
[f] Applied at 50% (v/v) antiserum load.

2.2. Adsorption kinetics

The mass balance equation formulation requires an independent description of the adsorption kinetics, i.e. an equation for $\partial Q/\partial t$ as a function of C. This is commonly obtained by fitting an adsorption isotherm equation to measured data. Although numerous expressions exist, the Langmuir isotherm

$$\frac{dQ}{dt} = k_1 C(Q_{max} - Q) - k_2 Q \quad (3)$$

is by far the most applied. Here, Q is the amount of target protein adsorbed, Q_{max} the maximum adsorption capacity, k_1 the adsorption constant, and k_2 the desorption constant. At equilibrium, the following relationship is obtained:

$$Q^* = \frac{Q_{max} C^*}{K_D + C^*} \quad (4)$$

where Q^* and C^* are the equilibrium concentrations of the adsorbed and bulk-phase target molecules respectively, and K_D is the equilibrium dissociation constant, i.e. k_2/k_1. This isotherm was originally developed for the next-neighbour independent monolayer adsorption of ideal gases [30]. Application of the model to protein solutes in a solvent makes the associated parameters dependent upon the state of the solvent. The assumptions behind the Langmuir isotherm are not strictly valid for proteins. Nevertheless, the Langmuir equation has been applied with reasonable success in many cases [1–3,5,6,8,9].

3. Materials and methods

3.1. Materials

The chromatographic and batch binding feedstocks (i.e., rabbit anti-human transferrin antiserum) were produced internally at DakoCytomation A/S (Glostrup, Denmark) following published procedures [31]. Pure rabbit Ig was available as a commercial product (X0903 concentrate and commercial product strength 20 g L^{-1}) at DakoCytomation A/S. The various chromatographic media employed, i.e.: rProtein A Sepharose FF and MabSelect^{TM} (GE Healthcare, Uppsala, Sweden); MabSorbent A1P (ProMetic BioSciences Ltd., Cambridge, UK); MBI HyperCel; MEP HyperCel; and MNA HyperCel (Pall Corporation, BioSepra Process Division Products and Services, Cergy-Saint-Christophe, France), were obtained as donations from the manufacturers (see Table 1 for detailed descriptions).

3.2. Preparation of adsorbents for batch binding studies

The adsorbents were thoroughly equilibrated by washing 3 times with at least 15 settled bed volumes of equilibration buffer (Table 3), before suction drying in a Buchner filter funnel lined with nylon support mesh (30–32 μm mesh size, Grønbech & Sønner A/S, Copenhagen, Denmark).

3.3. Preparation of feedstocks for batch binding studies and packed bed chromatography experiments

The feedstock used in all batch binding studies and chromatography experiments, was a rabbit anti-human transferrin antiserum that received no conditioning other than clarification, and in most cases dilution. Two hundred millilitre lots of crude rabbit antiserum pools from 'Danish Whites' were first filtered free of particulate matter by passage through 0.45 μm Nalgene disposable dead end membrane filters (VWR International, Buffalo Grove, IL, USA) to yield clarified undiluted antisera (hereafter designated '100% antiserum strength'). The mean Ig concentration from seven different batches of this feedstock was unusually high (21.2 ± 1.1 mg mL^{-1} *cf.* typically quoted value of 13.6 mg mL^{-1} for IgG [33]). In some chromatographic experiments these feedstocks were applied directly onto equilibrated packed beds, but in most cases they were diluted 2- , 3- or 5-fold with the appropriate column equilibration buffer (Table 3) to yield feeds with antiserum strengths of 50%, 33.3% or 20% (v/v), respectively.

Table 3
Packing and chromatographic conditions used for the matrices under test. A detailed description of chemicals and suppliers details is found in Bak [32]

Adsorbent	Packing/equilibration ($cm\,h^{-1}$)	Equilibration, loading[a] and washing buffer	Elution buffer	Regeneration solution
rProtein A Sepharose FF[b]	382/229	25 mM K–phosphate, pH 7	100 mM Na–citrate, pH 3.5	100 mM Na–citrate, pH 2.5
MabSelect[b]	611/229	25 mM K–phosphate, pH 7	100 mM Na–citrate, pH 3.5	100 mM Na–citrate, pH 2.5
MabSorbent A1P	Settling[c]/153	25 mM K–phosphate, pH 7	10 mM Na–citrate, pH 3	0.5 M NaOH
MEP HyperCel	Settling[c]/229	50 mM Tris–HCl, pH 8	50 mM Na–acetate, pH 4	1 M NaOH
MBI HyperCel	306/229	50 mM Na-acetate, 150 mM NaCl, pH 5.5	50 mM Tris–HCl, pH 9	1 M NaOH
MNA HyperCel	306/229	50 mM Na-acetate, 150 mM NaCl, pH 5.5	50 mM Tris–HCl, pH 9	1 M NaOH

[a] In all cases loading was performed at $38\,cm\,h^{-1}$, ensuring an 'on-column' time of 0.14–0.19 h. The choice of such a low flow rate was influenced by Pall's recommended residence time of 0.10–0.14 h for chromatography of antibodies on its hydrophobic charge induction media. The flow rates employed at all other stages (wash, elution, regeneration and test of theoretical plates) were the same as those employed for equilibration of the beds.

[b] The choice of starting buffers was influenced by experience at DakoCytomation A/S, combined with guidance from GE Healthcare 'Antibody Purification Handbook' (18-1037-46). The pH chosen for elution of 3.5 was determined after developing a previously 'loaded' packed bed of rProtein A Sepharose FF ($42\,mg\,Ig\,mL^{-1}$) with a pH gradient (starting at pH 7.0 and ending at pH 3.0). Complete desorption of rabbit Ig required a pH <3.8.

[c] Beds were first allowed to form by settling, before being packed down further at the equilibration flow rate.

3.4. Adsorption Isotherms with rabbit antisera

Various amounts (i.e. 25–674 mg) of the equilibrated suction dried adsorbents were mixed with 250–1400 μL aliquots of clarified (by passing through a 0.45 μm filter membrane) undiluted (100%, v/v) rabbit antiserum (with the exception of MabSorbent A1P, where 33% (v/v) antiserum was applied) yielding protein solution to suction dried gel ratios of 0.5–26 $\mu L\,mg^{-1}$. Binding was performed for 4 h at 20–23 °C while shaking at 1100 rpm on an IKA® Schüttler MTS vibrating shaker (IKA Labortechnik, Staufen, Germany) to ensure good mixing. Following binding, the supports were recovered by centrifugation at $2500 g_{av}$ for 600 s in an IEC MicroMax® Microcentrifuge (Gibco BRL, Life Technologies, Invitrogen, Carlsbad, CA, USA) and the resulting supernatants were analysed for Ig content as described in Section 3.7.1.

The equilibrium solid phase immunoglobulin concentrations, Q^*, were calculated indirectly using Eq. (5):

$$Q^* = \frac{(C_0 - C^*)V_{lq}}{m_s} \quad (5)$$

where C^* is the concentration of target protein measured in the supernatant, V_{lq} is the volume of protein solution, and m_s is the mass of suction dried adsorbent.

3.5. Adsorption kinetics

Clarified rabbit antisera prepared as described above (Section 3.3) was added to ~200 mg suction dried equilibrated adsorbent in Eppendorf tubes (900 μL per 200 mg of adsorbent). Binding was performed for 30 s–4 h at ambient temperature (21–23 °C) while shaking at 1100 rpm on an IKA® Schüttler MTS vibrating shaker (IKA Labortechnik, Staufen, Germany). Binding was terminated by high-speed pulse centrifugation in an IEC MicroMax® microcentrifuge (Gibco BRL, Life Technologies, Invitrogen, Carlsbad, CA, USA), and the supernatants were immediately transferred to new Eppendorf tubes. The resulting supernatants were analysed for Ig content as described in Section 3.7.1, and the determined Ig concentration was applied as C in Eq. (3).

3.6. Chromatography

All chromatography experiments were performed at ambient temperature employing an Äkta Explorer 100 chromatography system equipped with flow-through pH and conductivity probes, and a built-in fraction collector (GE Healthcare, Uppsala, Sweden). Approximately 5 mL packed beds of chromatographic media contained in 1 cm internal diameter columns (HR10/10, GE Healthcare) were operated under downward flow during packing, using flow rates similar to those recommended by the manufacturer of each matrix (MabSorbent A1P and MEP HyperCel beds were first allowed to form by settling, before being packed down further at the equilibration flow rate, Table 3). The flow adapters were then lowered onto the gels before copiously washing the beds with the appropriate equilibration buffer (Table 3) until the UV absorbance, conductivity, and pH of the liquid exiting the column reached that of the incoming equilibration buffer. The flow adaptors were then re-lowered onto the packed beds to give final bed heights between 5.8 and 7.3 cm. The buffer systems employed (Table 3) for media equilibration, product elution, and column regeneration of packed beds of the non-protein A based media were suggested by the individual media manufacturers. In the absence of clear recommendations from the maker's on buffer systems to use for any of the Protein A based matrices (i.e., rProtein A Sepharose FF and MabSelect), the following simple buffers were selected: 25 mM potassium phosphate, pH 7.0 for equilibration and washing, and 0.1 M sodium citrate, pH 3.5 for elution (Table 3).

A standard chromatographic run was performed in the following way. Packed beds of chromatography media were thoroughly equilibrated at flow rates between 153 and $229\,cm\,h^{-1}$, depending on the matrix under test, with an appropriate buffer (Table 3) until the UV absorbance, pH and conductivity of the flow exiting the column matched that entering it (i.e., at least 10 CV). Clarified antisera feedstocks were then loaded directly onto the

equilibrated packed beds at a linear flow rate of 38 cm h^{-1} in all cases, which guaranteed an 'on-column' residence time of 0.14–0.19 h (8.4–11.4 min.). On completion of sample loading, the columns were washed, eluted, regenerated, and stored in 20% (v/v) ethanol at ambient temperature (~21 °C). Between runs, the columns were probed for signs of bed deterioration [32]. Flow exiting columns was monitored continuously by on-line measurement of UV absorbance, pH and conductivity, and collected fractions (1–4 mL) were assayed for antibody contents as described in Section 3.7.1.

For dynamic breakthrough studies, the experimental approach taken was to sequentially challenge packed beds of each matrix with a series of different strengths (20–100%, v/v) of a clarified rabbit antiserum; beginning with the weakest and ending with the strongest. The beds were loaded with antiserum to well beyond the point of breakthrough; the total amount applied per mL of packed bed in each set of tests was kept relatively constant (i.e., at 60 ± 10 mg Ig mL^{-1} for beds of rProtein A Sepharose FF and Mabselect; 40 ± 4 mg Ig mL^{-1} for MEP HyperCel, MNA HyperCel, and MabSorbent A1P; 28 ± 6 mg Ig mL^{-1} for MBI HyperCel). Three of the matrices (MabSelect, MabSorbent A1P, MEP HyperCel) under test were challenged consecutively with rabbit antisera of 20%, 33%, 50%, and 100% (v/v) strength. The remaining three adsorbents (rProtein A Sepharose FF, MBI HyperCel, MNA HyperCel) were subjected to fewer (i.e. 1–3) and/or less testing (20–50%, v/v antiserum strength) runs.

3.7. Analysis

3.7.1. Immunoturbidimetric determination of rabbit immunoglobulin content

The assay for rabbit immunoglobulin applied in this study has been described in detail in [32,34] and is only briefly presented below. 'Purified immunoglobulin' (X0903, DakoCytomation A/S, Glostrup, Denmark) from non-immunised rabbits was diluted with dilution buffer 1 (S2005, a phosphate-buffered saline solution, pH 7.1–7.3, containing the preservative sodium azide, DakoCytomation A/S) to generate a series of standards with concentrations between 6.6 and 500 mg L^{-1}, and samples were appropriately diluted with the same buffer so as to lie within this range. Duplicate portions (50 μL) of diluted samples and standards were pipetted into the wells of a microtitre plate (96-well Polysorb, Nalgene Nunc Int., Rochester, NY, USA), followed by 90 μL aliquots of reaction buffer 2 (S2008, a solution composed of polyethylene glycol (PEG) polymers suspended in phosphate-buffered saline solution, pH 7.1–7.3, containing the preservative sodium azide, DakoCytomation A/S). After 5 s of brief mixing, the plate was incubated for ~300 s at 30 °C in a pre-heated $Thermo_{max}$ or Spectra Max 250 microtitre plate reader (Molecular Devices, Sunnyvale, CA, USA) and then read at 340 nm. Next, 210 μL aliquots of an antibody mixture consisting of 2-fold diluted goat anti-rabbit immunoglobulins (Z0421, DakoCytomation A/S) mixed in a 4:3 ratio with S2008 reaction buffer, were added rapidly to each well with a BioHit Proline 12-channel automated pipette (50–1200 μL, Helsinki, Finland). After incubating at 30 °C for 300 s the plates were re-read at 340 nm.

3.7.2. Computation

The Langmuir equation was fitted to the experimental data by adjusting k_1 and k_2, as described in more detail later. These two parameters were then applied in Eq. (1) to calculate the breakthrough curves. The partial differential equation was solved by an explicit finite difference technique. All initial value problems were solved with a fourth-order fixed step length explicit Runge/Kutta method.

4. Results and discussion

4.1. Parameter determination

Adsorption isotherms obtained for all adsorbents (Fig. 3) were found to fit the Langmuir type expression (Eq. (4)) well.

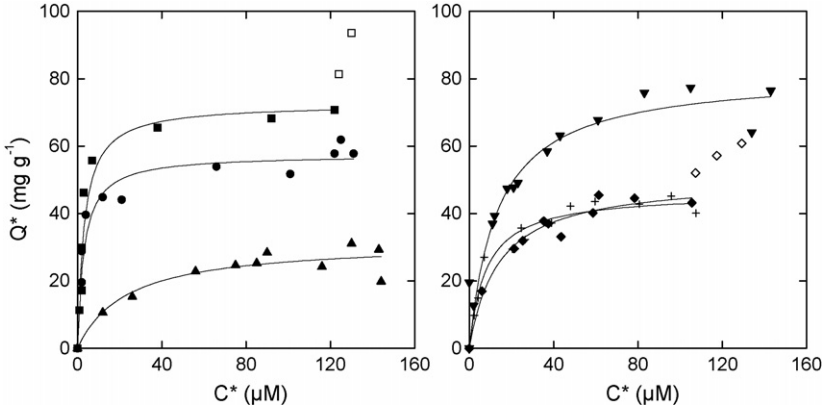

Fig. 3. Batch adsorption isotherms for equilibrium binding of rabbit Ig on six different chromatographic adsorbents after 4 h. In all batch experiments undiluted clarified feedstocks were applied, with the exception of MabSorbent A1P where 33.3% (v/v) diluted in equilibration buffer (Table 3) was applied to the equilibrated adsorbent: (■, □) rProtein A Sepharose FF; (● –) MabSelect; (▲ –) MabSorbent A1P; (▼ –) MEP HyperCel; (♦, ◊ –) MBI HyperCel; (+ –) MNA HyperCel. Open symbols were not included in the curve fit. The characteristic parameters of maximum capacity Q_{max} and K_D were determined from least square fits with Origin 4.1. These are listed in Table 2.

As indicated by Fig. 3, our data are the (C^*, Q^*) points. We determine K_D and Q_{max} by minimizing the sum of squared Q^*-residuals. This led to the Q_{max} and K_D values in Table 2.

For some of the adsorbents an upward kink, indicative of a transition from mono- to multi-layer adsorption [35,36], is observed at high equilibrium concentrations. As conditions giving rise to multi-layer adsorption, i.e. high 'antiserum to gel' concentration ratios, will not be reached in dynamic packed bed chromatographic experiments, only data points corresponding to monolayer binding were included in fits to the model.

For the rProtein A based adsorbents the K_D values are all an order of magnitude higher than is given by Horstmann and Chase [5], but very similar to those of Teng et al. [37] ($K_D = 2.74\ \mu M$). The 26% difference in Q_{max} in (Table 2) observed for the two Protein A based adsorbents (i.e., 72.5 mg g^{-1} for rProtein A Sepharose FF *cf.* 57.5 mg g^{-1} for MabSelect) correlates well with the respective ligand densities (Table 1) of the two supports (i.e., 6 mg mL^{-1} for rProtein A Sepharose FF *cf.* 5 mg mL^{-1} for MabSelect).

Generally, our K_D values seem higher than those previously reported for monocomponent systems. For MEP HyperCel, values of 0.29 μM [16] and 1.3 μM [34] have been determined, whereas for an analogue of MabSorbent A1P Teng et al. [37] reported a value of 5.06 μM. The high values found in this work with a complex feedstock *cf.* those with monocomponent systems [16,34,37] were not unexpected, given that all MT limitations are included in K_D with a lumped parameter approach [2,9], and Finette et al. [11] came up with similar findings in their single- versus multi-component surface adsorption study.

For the data fitting to the kinetic batch binding experiments, an Ig balance over the bulk liquid was written based on Eq. (3). This allows us to express C or equivalently the dimensionless C/C_0^* as a function of time. Treatments of the integration may vary. One can either solve the implied initial value problem numerically, or by analytical evaluation of the integral. We have done the latter, which gives us an explicit relationship between C/C_0^* and time, t. The parameters were determined in two different ways, i.e. by:

(i) independent determination of k_1 and k_2; and
(ii) determination of only k_1 or k_2 subject to the constraint $K_D = k_2/k_1$.

In both cases, our data are the C versus t points. In case (i), we determine k_1 and k_2 by minimizing the sum of squared C-residuals. That is, we adjust two parameters as if these were independent. In case (ii), we adjust only one, e.g. k_1, and express k_2 as $k_2 = K_D k_1$. One may also adjust k_2 and express k_1 as $k_1 = K_D/k_2$, but the two treatments are equivalent and give identical results. As shown in Fig. 4, these two different approaches gave almost super imposable curves for MabSelect and MabSorbent A1P. However, for the remaining adsorbents lower limiting values for C/C_0 were obtained from approach (ii) compared to approach (i). As shown in Table 2, the first approach resulted in a calculated K_D value ranging from 1.5 (for MabSorbent A1P) to 6.7 times higher (for MNA HyperCel). This is possibly an effect of mass transport limitations not accounted for in the model, confirmed by parametric studies showing that by applying a higher K_D (or a lower Q_{max}) resulted in the correct asymptotic value. In a pure affinity system, where immunoglobulin G (∼150 kDa) was adsorbed onto Protein A, good results could be obtained [5] describing the mass transport as discrete steps. In that study,

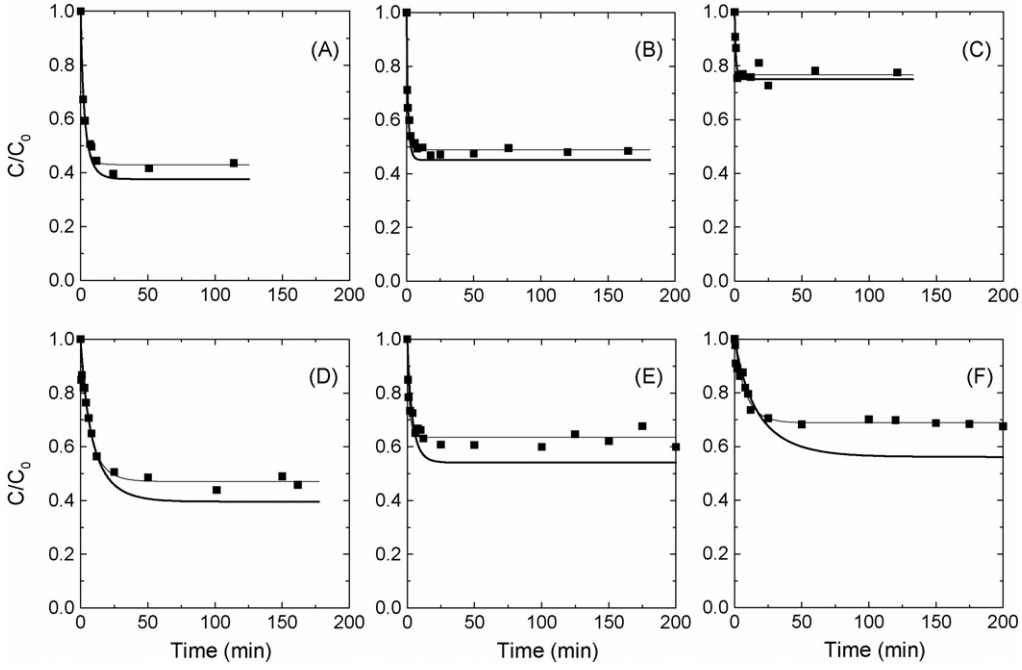

Fig. 4. Kinetics of batch adsorption of Ig from clarified rabbit antiserum to six chromatographic adsorbents. In all batch experiments undiluted clarified feedstocks were applied, with the exception of MabSorbent A1P where 33.3% (v/v) diluted in equilibration buffer (Table 3) was applied to the equilibrated adsorbent: (A) rProtein A Sepharose FF; (B) MabSelect; (C) MabSorbent A1P; (D) MEP HyperCel; (E) MBI HyperCel; (F) MNA HyperCel. Symbols are experimental data, and lines model predictions. Fine line: k_1 and k_2 as independent variables; Bold line: k_1 and k_2 as dependent variables.

pore diffusion was found to be the main parameter, and the best description of the batch adsorption was obtained by applying pore and film diffusion within the model. In a different investigation [4], where film and pore diffusion was rate limiting, it was not possible to obtain good fits when treating k_1 and k_2 as dependent parameters. Therefore, the discrepancy between the asymptotic value found and the experimental results, are possibly due to pore diffusion becoming the rate limiting mass transport mechanism, when the surface ligands are occupied.

It should be noted that the two modelled curves agree fairly well with the experimentally determined values during the first ~0.45 h (Fig. 4), except in the case of MBI HyperCel (Fig. 4E). As stated earlier, the objective of this study was to obtain a first approximation for Ig breakthrough, and not for the full breakthrough curve, where pore penetration, and other mass transport limitations, might become the rate limiting steps in later stages of adsorption. The 'on-column' contact time of the feedstock was 0.14–0.19 h in the performed experiments, and loading times were 0.67–1 h with initial breakthrough typically observed at 0.3–1 h. On this basis, it was assumed that the bulk part of the protein adsorption takes place within a thin layer at or near the adsorbent's surface. As a consequence, the fact that the modelled kinetic fit only followed the experimental results for the first 0.4 h was regarded as less of a problem.

4.2. Dynamic model

Dynamic simulations were performed with both sets of k_1 and k_2 determined for rProtein A Sepharose FF and MabSelect (Fig. 5). As expected, the best agreement between the predicted and the measured points was obtained with the parameters subjected to the constraint of K_D, with breakthrough being predicted a few minutes later than that of k_1 and k_2 as independent parameters.

As a result, the following simulations were all performed applying the parameters obtained for k_1 and k_2 as dependent variables, due to the lower K_D value (Table 2).

The above model was applied to four other adsorbents for purification of antibodies, comprising various synthetic low molecular weight ligands immobilised on hydrophilic porous supports. These included: MabSorbent A1P; MEP HyperCel; MBI HyperCel; and MNA HyperCel.

The model gave fair predictions of the Ig breakthrough curves on four of the six adsorbents (Fig. 6), i.e. rProtein A Sepharose FF, MabSelect, MabSorbent A1P, and to some extent MBI HyperCel. The simulated curves for MEP HyperCel and MNA HyperCel were parallel shifted and very shallow (Fig. 6D and F). The unusual shape of the curves is primarily due to the relatively low adsorption constant k_1, showing slow binding, i.e. instant partial breakthrough. Competitive binding on MEP HyperCel, between albumin and Ig [32] could be a possible explanation for the large discrepancy between the modelled and experimental data. This could be due to retarded Ig adsorption in the batch system, where the kinetic parameters were determined with 100% (v/v) antiserum, *cf.* the dynamic system experiments, which employed lower strength antiserum feedstocks, i.e. 20, 33, and 50% (v/v). Finally, the shape of the experimental breakthrough curve is similar to what has been reported for other displacing systems [38,39].

MNA HyperCel shows the same pattern (Fig. 6F), with a very shallow modelled curve, indicative of competitive binding as with MEP HyperCel. However, this is yet to be supported by further experiments.

Apart from MNA HyperCel and MEP HyperCel, a general trend was that the model underestimated the experimentally obtained frontal analysis, for four of the six adsorbents, namely rProtein A Sepharose FF, MabSelect, MabSorbent A1P, and MBI HyperCel. Interestingly, when the Q_{max} values were raised by a factor of 1.25 good fits were obtained to the rProtein A Sepharose FF, MabSelect, and MabSorbent A1P data at all antiserum concentrations employed (Fig. 7). Skidmore et al. [4] have likewise experienced an underestimation of Q_{max}, by 15% in their case, for the adsorption of albumin on an ion-exchanger, in a model where film and pore diffusion were rate determining. Generally, the model predictions are below 0.5 C/C_0. This can be expected, given that intra-particle mass transport characteristics become more important, the longer the residence time the immunoglobulins have on the column.

MBI HyperCel also showed good agreement between the modelled values and the experimental results at 50% (v/v) anti-

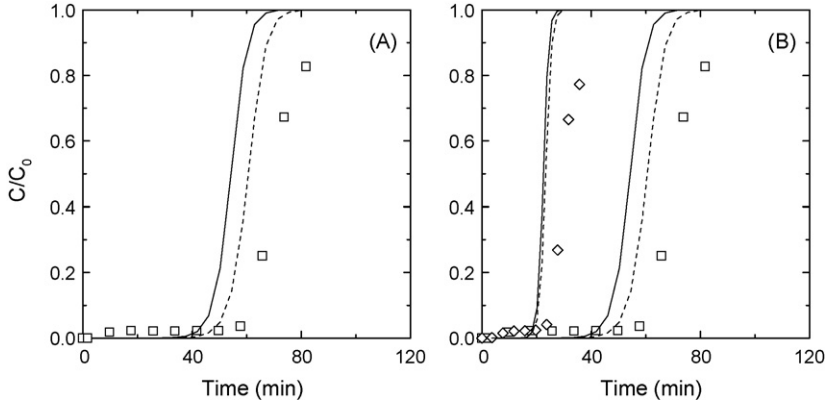

Fig. 5. Breakthrough curve for rabbit Ig after loading 33% (v/v) (□) and 100% (v/v) (◊) clarified rabbit antiserum to packed beds of: (A) rProtein A Sepharose FF; and (B) MabSelect. Symbols are experimental data and lines model predictions: (—) k_1 and k_2 as independent variables; (- -) k_1 and k_2 as dependent variables (Table 2). For sake of clarity, only 100% and 33% (v/v) antiserum feedstock were included for MabSelect. Q_{max}, L and ε for each adsorbent are tabulated in Table 2.

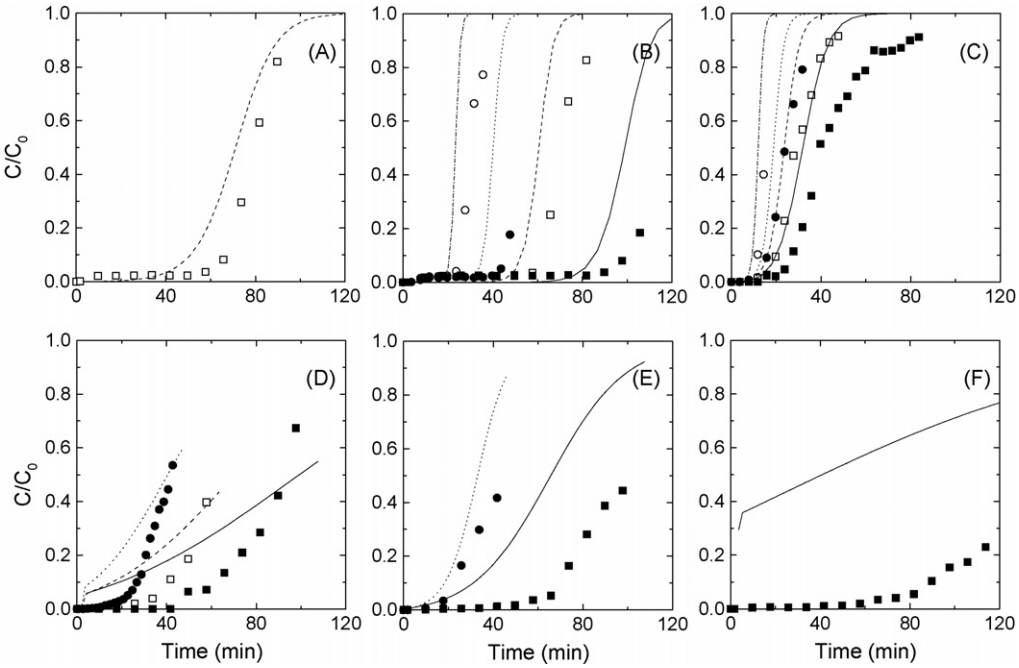

Fig. 6. Breakthrough curves for rabbit Ig after loading 20–100% (v/v) clarified rabbit antiserum to packed beds of: (A) rProtein A Sepharose FF; (B) MabSelect; (C) MabSorbent A1P; (D) MEP HyperCel; (E) MBI HyperCel; (F) MNA HyperCel. Symbols are experimental data and lines model predictions with varying feedstock antiserum strength: (— ■:) 20% (v/v); (– – □): 33.3% (v/v); (. . . ●): 50% (v/v); (–·–·–·◯): 100% antiserum. Q_{max}, L and ε for each adsorbent are tabulated in Table 2.

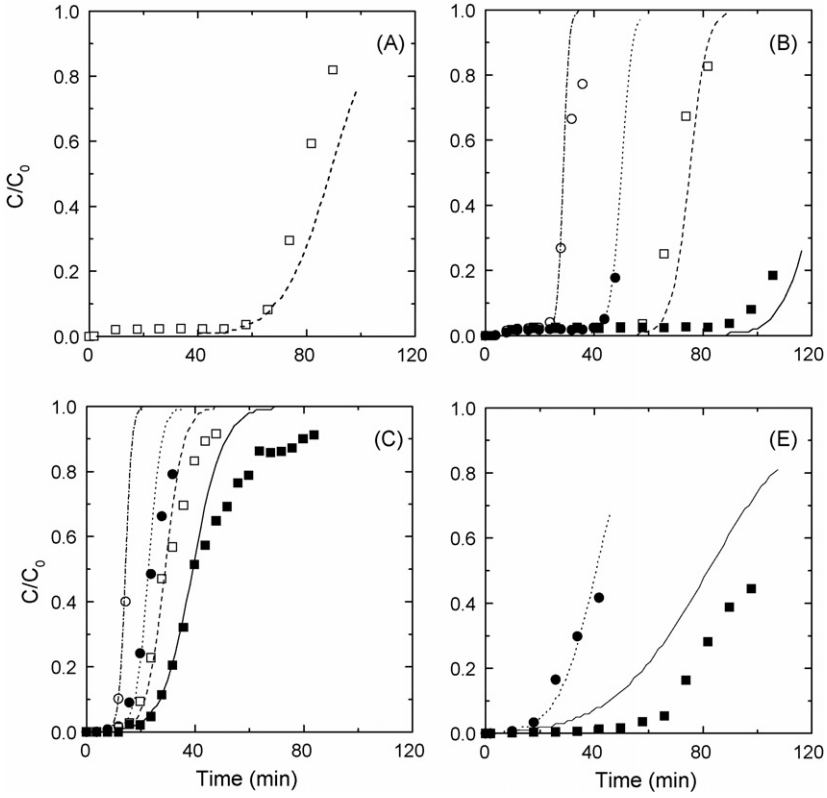

Fig. 7. Normalised breakthrough curves for rabbit Ig after loading 20–100% (v/v) clarified rabbit antiserum to packed beds of: (A) rProtein A Sepharose FF; (B) MabSelect; (C) MabSorbent A1P; (E) MBI HyperCel. Symbols are experimental data and lines model predictions with varying feedstock antiserum strength: (— ■:) 20% (v/v); (– – □): 33.3% (v/v); (. . . ●): 50% (v/v); (–·–·–· ◯): 100%. The values of L and ε employed for each adsorbent are cited in Table 2, whereas the Q_{max} values cited in Table 2 were raised by a factor of 1.25-fold.

serum, when applying the 25% increase to Q_{max}, whereas a parallel shift toward the origin of the predicted values is seen for 20% (v/v) antiserum (Fig. 7E). The slope of the curve is correct, which, if following the analogy for MEP HyperCel presented above, is indicative of competition between contaminating molecules and Igs. However, contrary to MEP HyperCel, Ig adsorption to MBI HyperCel is salt-dependent [32], a parameter, which has not been included in this model (based on Langmuir adsorption kinetics). The good fit at 50% (v/v) antiserum is therefore, possibly due to the ionic strength being closer to that at 100% (v/v) antiserum, at which the kinetic parameters were determined.The delayed breakthrough found from a 25% increase in Q_{max}, is a consequence of the model's form. If more per loaded amount of material (i.e. have greater Q_{max}) can be bound then breakthrough will be delayed. Breakthrough calculations require an expression for the binding rate ($\partial Q/\partial t$) as a function of concentration (C). This expression requires parameters k_1, k_2, and Q_{max}. Therefore, if we can assume the validity of the model the reliability of the predicted breakthrough depends directly on the quality of these parameters. Ideally, a unique set of optimal parameters exists, but unfortunately, realistic data reduction cannot yield a unique set of parameters. Q_{max} and K_D (Fig. 3) are determined from measured data combined with a mathematical minimization procedure. If the measured data are changed, Q_{max} and K_D will likewise change. A crucial issue is the sensitivity of Q_{max} and K_D to variations in the input data. In the case of rProtein A Sepharose FF (squares) the open symbols are not included in the curve fit. If the open squared symbols in upper right corner were included in the fit, the values of K_D and Q_{max} would clearly be altered. For reasons mentioned earlier, we chose not to include these data in the fit. Clearly, more precise knowledge of experimental uncertainties would be valuable in assisting such decision-making.

Information on parameter uncertainty in given models can be extracted, and is related to the inverse of the optimization problems second derivative matrix. Nonlinear minimization problems in which the objective function is a sum, s, of m squared residuals (with n parameter values, x) are often solved using what is equivalent to a linear approximation to the residuals [40]. If the objective function is $s(\boldsymbol{x}) = \boldsymbol{r}^T\boldsymbol{r}$, where $\boldsymbol{x}$ is $n \times 1$, then derivatives of s are given by $\boldsymbol{g}(\boldsymbol{x}) = 2\boldsymbol{A}\boldsymbol{r}$ where $\boldsymbol{A}$ is the $n \times m$ Jacobian matrix and where the second derivatives matrix is given approximately by linearization as $\boldsymbol{G} = 2\boldsymbol{A}\boldsymbol{A}^T$. The inverse of $\boldsymbol{A}\boldsymbol{A}^T$ is a multiple of the variance-covariance matrix, $\boldsymbol{D}$, which can be shown to satisfy $\boldsymbol{D} = \sigma^2(\boldsymbol{A}\boldsymbol{A}^T)^{-1}$. The diagonal elements of $\boldsymbol{D}$ give the variances of x. It can also be shown that an estimator for σ^2 is $\hat{s}/(m-n)$ where $\hat{s}$ is the sum of squares obtained by minimizing s. This fact enables the variance-covariance matrix to be determined and gives useful statistical information about the distribution of the least squares solution. In general, the smoother the fit, the less sensitive the parameters will be. On the other hand, if there is scatter, great variance results. To illustrate this point we draw the reader's attention to the data in Fig. 3. Here, a parameter variance of the order 25% of the parameter value would not be unreasonable. For example, in the case of the MEP HyperCel data (down-triangles, right hand side panel of Fig. 3), one data point (coordinates $Q^* = 64\ m\ g^{-1}$; $C^* = 134\ \mu M$) appears to be somewhat outlying. This point is not necessarily in error, it could be that all four triangles in the right end of the figure are just scattered. However, if this point were to be removed from the regression, the fit curve representing the data set would clearly be shifted upward.

In the present case, reiteration of the data reduction based on knowledge of the experimental breakthrough behaviour might provide better parameters and as a consequence, breakthrough behaviour in better agreement with experiment.

5. Conclusions

A model has been developed, which accurately predicts the initial Ig breakthrough in frontal chromatographic analysis of direct capture of rabbit Ig from clarified rabbit antiserum in strengths of 20–100% (v/v) (Fig. 7). Based on a lumped parameter approach, the model employs Langmuir adsorption parameters, determined in batch binding studies with 'neat' (i.e. 100% v/v) clarified rabbit antiserum.

In the current study, the Langmuir parameters were determined at 100% (v/v) antiserum. Generally superior fits of the model predictions were seen at 100% (v/v) antiserum, with the predictive power diminishing at lower strengths. Contrary to this, MabSorbent A1P measurements agreed excellently with the model predictions at all strengths. This finding probably originates from the numerically very low changes in binding capacity relative to the antiserum strength [32,41]. As feedstock ionic strength differences can influence binding capacities on a range of adsorbents, a modified Langmuir model accounting for the reduced ionic strength at antiserum strengths less than 100% (v/v) could be applied. Such a modification has been developed for ion-exchangers and dye-ligand chromatography [42], based on empirical data, but the increased requirements for parameter determination necessitated by this modification impart reduced appeal, given the original objective in this study of keeping the model simple.

Confocal microscopy has been applied for *in situ* studies of the dynamics of protein adsorption of binary protein mixtures, comprising albumin and IgG, during batch adsorption [43] and packed bed chromatography [42] on ion-exchangers and rProtein A affinity chromatography media. These studies have revealed that protein adsorption on ion-exchangers shows altered selectivity during the various chromatographic stages, leading to a suggested "apparent optimum in adsorption selectivity" [43], whereas no displacement was observed on the affinity chromatography media. This implies that in complex protein systems involving displacement phenomena, a time-parameter should be included in any model, as steady state kinetic parameters from batch adsorption experiments will fail to reflect these aspects of protein adsorption.

In the current study, very similar values for packed bed voidages were determined, based on a settled bed voidage of 0.4. Alternatively, the bed voidage could be determined by exclusion techniques, applying dextran or latex particles, but as the objective of this study was to obtain a first estimate of capture performance without operating a column, we feel this is not necessary. Therefore, it is proposed that for soft adsorbents packed

at industrially applied flow rates a packed bed voidage of $\varepsilon = 0.3$ is employed as a first estimate.

Nomenclature

ε	packed bed voidage fraction (—)
ε_0	settled bed voidage fraction (—)
σ^2	mean error of a determination whose weight is unity
A	$(n \times m)$ Jacobian matrix
A_s	symmetry factor (—)
C	concentration of target molecule in bulk liquid ($mg\,L^{-1}$)
C^*	concentration of target molecule in bulk liquid at equilibrium ($mg\,L^{-1}$)
D	variance-covariance matrix
g	derivatives of objective function
G	second derivatives matrix as given approximately by linearization
k_1	adsorption constant ($L\,kg^{-1}\,h^{-1}$)
k_2	desorption constant (h^{-1})
K_D	equilibrium dissociation constant (μM)
Q^*	equilibrium adsorption capacity ($mg\,g^{-1}$, $mg\,mL^{-1}$)
Q_{max}	maximum adsorption capacity ($mg\,g^{-1}$, $mg\,mL^{-1}$)
r	residuals
s	objective function value
$\hat{s}$	value of objective function at minimum
t	time (s, h)
u	superficial fluid velocity ($m\,h^{-1}$)
V	packed bed volume (mL)
V_0	settled bed volume (mL)
V_R	retention time (mL)
V_S	volume of particles in bed (m^3)
V_T	total bed volume (m^3)
$w_{1/2}$	peak with at half height (mL)
x	model parameter array $(n \times 1)$
z	bed height (m)

References

[1] O. Mendieta-Taboada, E.S. Kamimura, F. Maugeri, Biotechnol. Lett. 23 (2001) 781.
[2] H.A. Chase, J. Chromatogr. 297 (1984) 179.
[3] J.A. Noriega, A. Tejeda, I. Magaña, J. Ortega, R. Guzman, Biotechnol. Prog. 13 (1997) 296.
[4] G. Skidmore, B.J. Horstmann, H.A. Chase, J. Chromatogr. 498 (1990) 113.
[5] B.J. Horstmann, H.A. Chase, Chem. Eng. Res. Des. 67 (1989) 243.
[6] B.J. Horstmann, H.A. Chase, Bioseparation 7 (1998) 145–157.
[7] P.M. Doran, Bioprocess Engineering Principles, Academic Press, 1995.
[8] W.-D. Chen, X.-Y. Dong, Y. Sun, J. Chromatogr. A 962 (2002) 29.
[9] G.M.S. Finette, Q. Mao, M.T.W. Hearn, J. Chromatogr. A 763 (1997) 71.
[10] G.L. Skidmore, H.A. Chase, J. Chromatogr. A 505 (1990) 329.
[11] G.M.S. Finette, B.S. Baharin, Q. Mao, M.T.W. Hearn, Biotechnol. Prog. 13 (3) (1997) 265.
[12] C.R. Lowe, A.R. Lowe, G. Gupta, J. Biochem. Biophys. Methods 49 (2001) 561.
[13] E. Boschetti, D. Judd, W.E. Schwartz, P. Tunon, Genet. Eng. (N. Y.) 20 (13) (2000) 34.
[14] E. Boschetti, Trends Biotechnol. 20 (8) (2002) 333.
[15] S.C. Burton, D.R.K. Harding, J. Biochem. Biophys. Methods 49 (2001) 275.
[16] L. Guerrier, I. Flayeux, E. Boschetti, J. Chromatogr. B 755 (2001) 37.
[17] W. Schwartz, D. Judd, M. Wysocki, L. Guerrier, E. Birk-Wilson, E. Boschetti, J. Chromatogr. A 908 (2001) 251.
[18] A. Ljunglöf, J. Thömmes, J. Chromatogr. A 813 (1998) 387.
[19] M.T.W. Hearn, B. Anspach, Sep. Purif. Methods 30 (2) (2001) 221.
[20] P.V. Danckwerts, Chem. Eng. Sci. 2 (1) (1953) 1.
[21] F. Carlsson, A. Axelsson, G. Zacchi, Comp. Chem. Eng. 18 (Suppl.) (1994) S657.
[22] E. Pålsson, A. Axelsson, P.O. Larsson, J. Chromatogr. A 912 (2001) 235.
[23] J.J. Stickel, A. Fotopoulos, Biotechnol. Prog. 17 (4) (2001) 744–751.
[24] J. Thömmes, A. Bader, M. Halfar, A. Karau, M. Kula, J. Chromatogr. A 752 (1996) 111.
[25] E. Pålsson, P. Gustavsson, P.O. Larsson, J. Chromatogr. A 878 (2000) 17.
[26] N.A. Willoughby, R. Hjorth, N.J. Titchener-Hooker, Biotechnol. Bioeng. 69 (6) (2000) 648.
[27] F.H. Arnold, H.W. Blanch, C.R. Wilke, Chem. Eng. J. 30 (1985) B25.
[28] P.M. Boyer, J.T. Hsu, Chem. Eng. Sci. 47 (1) (1992) 241.
[29] F. Svec, J.M.J. Fréchet, Science 273 (1996) 205.
[30] P.W. Atkins, Physical Chemistry, fourth ed., Oxford University Press, Oxoford, 1990.
[31] N.M.G. Harboe, A. Ingild, Scand. J. Immunol. 17 (suppl. 10) (1983) 345–351.
[32] H. Bak, PhD Thesis, Technical University of Denmark, 2004, ISBN 87-88584-99-2.
[33] R. Lindmark, K. Thorén-Tolling, J. Sjöquist, J. Immunol. 62 (1) (1983) 1.
[34] H. Bak, J. Kyhse-Andersen, O.R.T. Thomas, J. Chromatogr. B 848 (2007) 142.
[35] W. Norde, Adv. Colloid Interface Sci. 25 (1986) 267.
[36] A. Heebøll-Nielsen, PhD Thesis, Technical University of Denmark, 2002, ISBN 87-88584-82-8.
[37] S.F. Teng, K. Sproule, A. Husain, C.R. Lowe, J. Chromatogr. B 740 (2002) 1.
[38] J. Hubbuch, T. Linden, E. Knieps, J. Thömmes, M.-R. Kula, Biotech. Bioeng. 80 (4) (2002) 359.
[39] W. Weinbrenner, M.R. Etzel, J. Chromatogr. A 662 (1994) 414.
[40] R. Fletcher, Practical Methods of Optimization, second ed., Wiley, Bath, UK, 2000.
[41] H. Bak, O.R.T. Thomas, J. Chromatogr. B 848 (2007) 116.
[42] Q. Lan, A.S. Bassi, J.-X. Zhu, A. Margaritis, Chem. Eng. J. 81 (2001) 179.
[43] T. Linden, A. Ljunglöf, M. Kula, J. Thömmes, Biotechnol. Bioeng. 65 (6) (1999) 622.